

## Original Article

# Apelin is essential for the development of laser-induced choroidal neovascularization model

Jian Jiao<sup>1,2</sup>, Yan Song<sup>3</sup>, Dong Qin<sup>1</sup>, Yanrong Jiang<sup>1</sup>

<sup>1</sup>Department of Ophthalmology, People's Hospital, Peking University; Key Laboratory of Vision Loss and Restoration, Ministry of Education; Beijing Key Laboratory of Diagnosis and Therapy of Retinal and Choroid Diseases, Beijing, China; <sup>2</sup>Department of Ophthalmology, Beijing Chaoyang Hospital, Capital University of Medical Sciences, Beijing, China; <sup>3</sup>Department of Pathology, Cancer Institute and Hospital, Chinese Academy of Medical Sciences, and Peking Union Medical College, Beijing, China

Received January 26, 2016; Accepted April 23, 2016; Epub February 1, 2017; Published February 15, 2017

**Abstract:** The apelin was reported to be involved in angiogenesis. This study investigated its role in the development of experimental choroidal neovascularization (CNV) model. Lentivirus-mediated short hairpin RNA (shRNA) targeting the rat apelin gene (Apelin-RNAi-LV) and control shRNA (NC-RFP-LV) were designed and employed. Experimental CNV rat models induced by laser photocoagulation were randomly assigned to be intravitreally injected with phosphate-buffered saline (PBS), NC-RFP-LV and Apelin-RNAi-LV. The expression of apelin was evaluated by RT-PCR analysis, western-blot analysis, and immunofluorescence staining. The laser-induced CNV tissue was assessed qualitatively and quantitatively by histopathological sections, fundus fluorescein angiography, and choroidal flat mounts. The gene expression of apelin was upregulated during CNV formation in a time-dependent manner. By silencing the apelin gene, the expression of apelin was downregulated significantly, and the laser-induced CNV was inhibited obviously. Our study suggests that the apelin may play an important role in the development of laser-induced CNV, and it may act as a novel therapeutic option to inhibit CNV formation.

**Keywords:** Apelin, choroidal neovascularization, rat

## Introduction

Choroidal neovascularization (CNV) occurs in many diseases such as wet age-related macular degeneration (AMD), pathological myopia, and angioid streaks [1]; particularly, AMD is the leading cause of blindness in the industrialized countries [2]. Therefore, various experimental CNV models have been developed to investigate its molecular mechanism [1, 3, 4]. A reliable way to induce CNV in animals is to rupture the Bruch's membrane by laser photocoagulation.

Studies have demonstrated that the key to the neovascular response is the production of vascular endothelial growth factor (VEGF). However, despite the improvements offered by current anti-VEGF therapies, it is necessary to explore new and additional factors involved in CNV. Fortunately, many factors apart from VEGF have already been found to play a role in CNV [5-7]. Apelin is an endogenous ligand for

the angiotensin-1-like receptor APJ [8], and it is reported to act as an angiogenic factor that can stimulate the proliferation and migration of retinal vessel endothelial cells (ECs) and accelerate vascular tube formation [8, 9], and this function cannot be replaced by VEGF [10]. Furthermore, recent studies have reported that apelin may be involved in retinal neovascularization during the development of proliferative diabetic retinopathy [11, 12], and apelin is a prerequisite factor for hypoxia-induced retinal angiogenesis independent of the VEGF/VEGF receptor signaling pathway [13].

Since apelin is recognized as a factor promoting angiogenesis, and the role of apelin in CNV has not been well demonstrated, we designed this study. We used the lentivirus vector system to deliver a specially designed short hairpin RNA (shRNA) targeting the rat apelin gene to evaluate the potential role of the apelin in the development of laser-induced CNV.

## Materials and methods

### Animals

We purchased normal male Brown-Norway (BN) rats (weight ranged from 200 g to 250 g) from Vital River Laboratories (Beijing, China). The present study followed the Guide of ARVO Statement for the Use of Animals in Ophthalmic and Vision Research, and was approved by Peking University People's Hospital Ethics Committee.

### Lentivirus vectors for shRNA

Lentivirus-mediated shRNA targeting the rat apelin gene (Apelin-RNAi-LV; 5'-CACAGATGAGTTCTCTTCTCT-3'), and the control shRNA encoding the red fluorescent protein (RFP) sequence (NC-RFP-LV; 5'-TTCTCCGAACGTGTCA-CGT-3') were constructed from lentivirus vector by Genechem Co., Ltd., Shanghai, China. The selectivity of the shRNA was confirmed by sequencing the product of PCR, and was determined to be unique to the rat gene by Basic Local Alignment Search Tool searches of the GenBank database. Apelin-RNAi-LV and NC-RFP-LV were produced in 293 t packaging cells and titered to  $9 \times 10^8$  TU/mL. Finally, they were transduced into IEC-6 cells to test the transfection efficiency.

### Laser-induced CNV

Rats were anesthetized by the intraperitoneal injection of pentobarbital (30 mg/kg), and the pupils were dilated with tropicamide (5 mg/mL) and phenylephrine hydrochloride (5 mg/mL). Laser photocoagulation was performed on the right eyes: 8 spots were photocoagulated between the retinal vessels in a peripapillary distribution at a distance of approximately 2 disc diameters. For this, the following laser parameters were used: 200 mW, 100  $\mu$ m, 521 nm, and 50 ms (Coherent Novus 2000, USA). Only a laser lesion with a subretinal bubble indicating perforation of Bruch's membranes was considered effective and thus included in the study. These rats were then randomly sorted into 3 equal groups.

### Intravitreal injections

Immediately after photocoagulation, 5  $\mu$ L of either PBS (Vehicle group), NC-RFP-LV (NC

group), or Apelin-RNAi-LV (RNAi group) was injected intravitreally to the photocoagulated eyes using a micro-injector (Hamilton Co., USA) with a 30-gauge needle under a microscope.

### Fundus fluorescein angiography (FFA)

FFA was carried out to evaluate CNV development and its score on days 3, 7, 14, 21, and 28 after laser photocoagulation. After the pupils were dilated, the anesthetized rats were intraperitoneally injected with 10% fluorescein sodium (0.1 mL/kg). Early-phase angiograms were obtained within 1-3 min after injection by a digital fundus camera (TRC 50DX, Topcon, Tokyo, Japan). Two experienced observers processed and scored the images. The CNV formation was evaluated according to the scoring described previously by Semkova [14]. The guidelines for CNV scoring were as follows: no leakage (score 0); minimum leakage or staining of tissue with no leakage (score 1); small but evident leakage less than one-fourth of the disc area (score 2); large evident leakage (score 3).

### Semiquantitative RT-PCR analysis

Three rats from every group on days 3, 7, 14, 21, and 28 after laser photocoagulation were euthanatized, and the photocoagulated eyes were enucleated immediately to extract the total RNA. The total RNA was extracted from the RPE-choroid-sclera complex using Trizol (Invitrogen, USA) and converted to cDNA using a Revert Aid First Strand cDNA Synthesis Kit (Fermentas, Canada). The amplification program was 95°C for 10 min, followed by 95°C for 10 s, and followed by 60°C for 30 s, for 40 cycles. The primers for rats were as follows: GAPDH sense, 5'-TTCAACGGCACAGTCAAGG-3'; GAPDH antisense, 5'-CTCAGCACAGCATCACC-3'; apelin sense, 5'-GGCTAGAAGAAGGCAACATGC-3'; apelin antisense, 5'-CCGCTGTCTGCGAA-ATTCCT-3'. After amplification, the samples were electrophoresed on a 2% agarose gel (Sigma, USA) in TBE containing 0.4 mg/mL ethidium bromide (Sigma, USA), and the bands were photographed using a bioimaging system (EC3™ Imaging System, USA). The relative abundance of the product was assessed as the ratio of the aimed gene band to the GAPDH band for each sample by using ImageJ software (National Institutes of Health, USA). The experiments were repeated three times with similar results.

## Apelin is essential for CNV

### *Semiquantitative western-blot analysis*

Three rats from every group on days 3, 7, 14, 21, and 28 after laser photocoagulation were euthanized, and the photocoagulated eyes were enucleated immediately to extract the total protein from the RPE-choroid-sclera complex. The protein content of each lysate was measured using a BCA Protein Assay Kit (Pierce, USA). Equivalent amounts (20 µg) of protein were electrophoresed on 15% sodium dodecyl sulfate-polyacrylamide gels, and the separated proteins were transferred to polyvinylidene difluoride membranes (Millipore, USA). The blots were blocked with 5% skim milk powder in TBST and probed overnight at 4°C with primary antibodies against apelin (1:300, Abcam, UK), or β-actin (1:3000; Boster, China). After the membranes were washed with TBST, horseradish peroxidase-conjugated secondary antibodies (1:5000; Boster, China) were incubated with the membranes for 1 h at room temperature. Finally, proteins were detected by using a Chemiluminescent HRP Substrate (Millipore Corporation, USA) and visualized after film exposure (XBT-1, Kodak, China). The protein levels were quantified by densitometry and the ratio to β-actin levels by using ImageJ software (National Institutes of Health, USA). The experiments were repeated three times with similar results.

### *Histopathology*

Three rats from every group were euthanized on days 3, 7, 14, 21, and 28 after laser photocoagulation. The photocoagulated eyes were enucleated immediately, embedded in an optimum cutting temperature compound (Tissue-Tek, Sakura Finetek Inc., Japan) and directly frozen in cryostat (Leica CM1900, Germany) at -20°C. Serial 6 µm frozen sections were cut along the vertical meridian and crossing the center of the laser lesion, air-dried, and stained with hematoxylin and eosin (H-E) staining. The histopathological sections were photographed using a microscope (Eclipse 50i, Japan) with a digital camera, and the maximum CNV thickness was measured by using ImageJ software (National Institutes of Health, USA).

### *Immunofluorescence staining*

Serial 6 µm frozen sections were used for immunofluorescence staining. After being blocked

for 2 h in PBS containing 5% bovine serum albumin and 1% Triton X-100, the sections were incubated with primary antibodies against apelin (1:150, Abcam, UK), CD105 (1:150, CapitalBio, China) overnight at 4°C. For negative controls, the primary antibodies were replaced with PBS. After rinsing in PBS, the slides were incubated with fluorescein isothiocyanate (FITC) or TRITC-labeled secondary antibodies for 1 h at room temperature and counterstained with 4',6-diamidino-2-phenylindole (DAPI, Invitrogen, USA) to label the nucleus. Finally, the sections were photographed under fluorescence microscope (Eclipse 50i, Nikon, Japan).

### *FITC-dextran labeled choroid flat mounts*

Three rats from every group on days 7, 14, 21, and 28 after laser photocoagulation were used for the choroidal flat mounts by the method described previously by Edelman [15]. Briefly, the rats were anesthetized and perfused with 1 mL PBS containing 50 mg/mL FITC-dextran ( $2 \times 10^6$  average molecular weight; Sigma, USA) through the left ventricle. The photocoagulated right eyes were enucleated and fixed in 4% paraformaldehyde for 1 h at room temperature. The anterior segment and sensory retina were carefully removed. Four to six radial relaxing incisions were made from the edge to the equator to allow the remaining RPE-choroid-sclera complex to be flattened on a glass slide with the RPE facing up. The flat mounts were photographed by laser confocal microscopy (LSM700; Carl Zeiss, Germany), and then areas of CNV were measured using ImageJ software (National Institutes of Health, USA).

### *Statistical analysis*

All values are presented as mean ± SD and compared by one-way analysis of variance (ANOVA) and Dunnett's multiple comparison test with SPSS V13.0 (SPSS Inc., USA).  $P < 0.05$  was considered statistically significant.

## Results

### *Upregulation of apelin in the laser-induced CNV model*

Apelin was reported to act as an angiogenic factor and exerted its activity by combining with its receptor APJ. As a result, we first tried to

## Apelin is essential for CNV

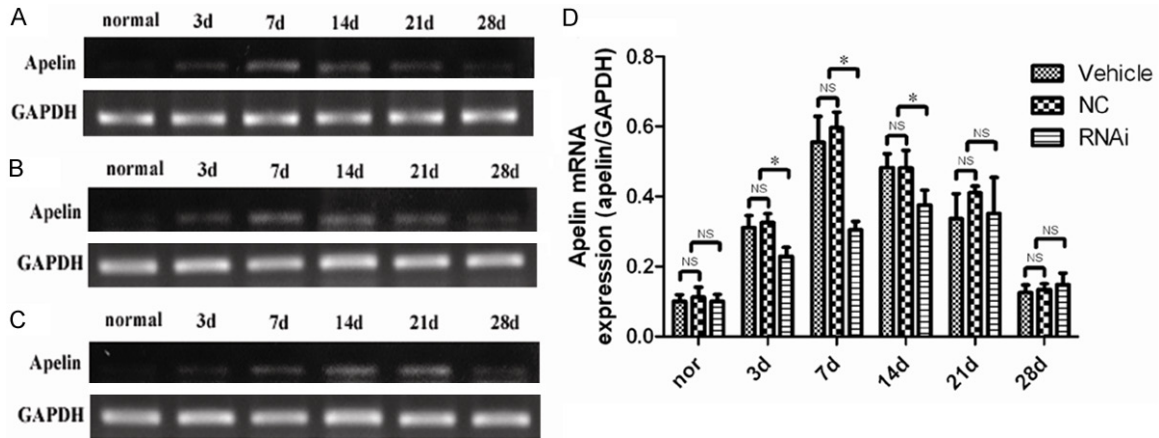


**Figure 1.** Expression of apelin by RT-PCR analysis in the laser-induced CNV model from day 3 to day 28 after photocoagulation. The mRNA levels of apelin was upregulated in the Vehicle group (A, D) and NC group (B, D), and suppressed in the RNAi group (C, D) after the intravitreal injection of Apelin-RNAi-LV. \* $P < 0.05$ .

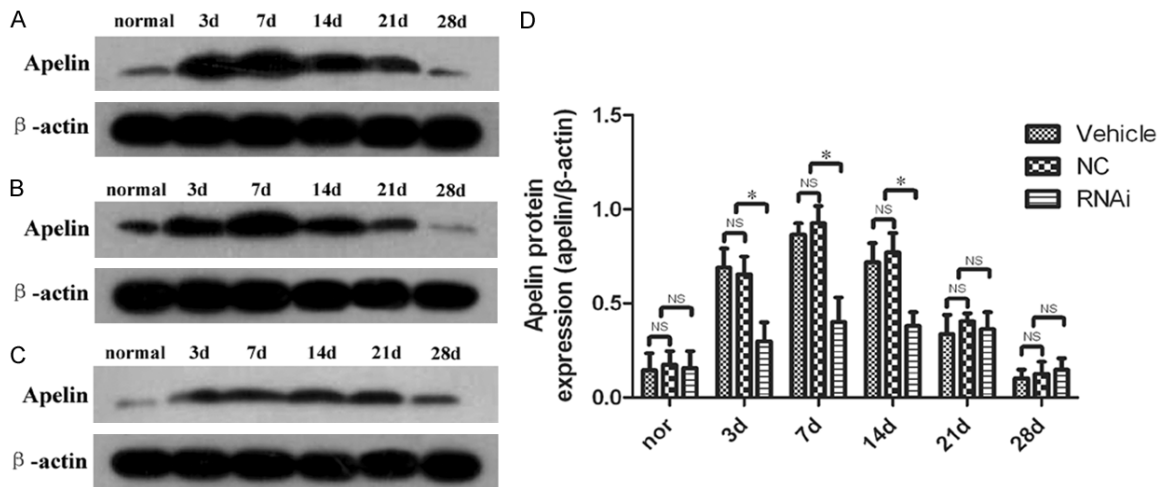


**Figure 2.** Expression of apelin by western-blot analysis in the CNV model from day 3 to 28 after photocoagulation. The protein levels of apelin was upregulated in the Vehicle group (A, D) and NC group (B, D), and suppressed in the RNAi group (C, D) after the intravitreal injection of Apelin-RNAi-LV. \* $P < 0.05$ .

demonstrate the expression of apelin in the laser-induced CNV model (Vehicle group) by semi-quantitative RT-PCR and western-blot analysis. RT-PCR analysis revealed that apelin mRNA levels increased on day 3 after photocoagulation, reached a maximum on day 7, and then decreased (Figure 1A, 1D). The protein level of apelin also showed a similar tendency (Figure 2A, 2D).

### *Tissue localization of apelin in the CNV model by immunofluorescence staining*

Experiments were performed to investigate which type of cells apelin was located in by immunofluorescence staining. Studies had reported that CD105 was a marker of activated ECs.

The colocalization of apelin and CD105 showed that apelin was expressed in the activated ECs of CNV tissue (Figure 3A-E; the method that yielded these merged pictures, see Figure S1A-I). The expression of apelin was observed in the lesions on day 3 after photocoagulation (Figure 3A), reached the maximum on day 7 (Figure 3B), and then decreased (Figure 3C-E), which seemed to be in accordance with the results from the RT-PCR and western-blot analysis.

### *Suppression of apelin gene expression by Apelin-RNAi-LV*

Experiments were next performed to determine whether shRNA targeting the rat apelin gene

## Apelin is essential for CNV

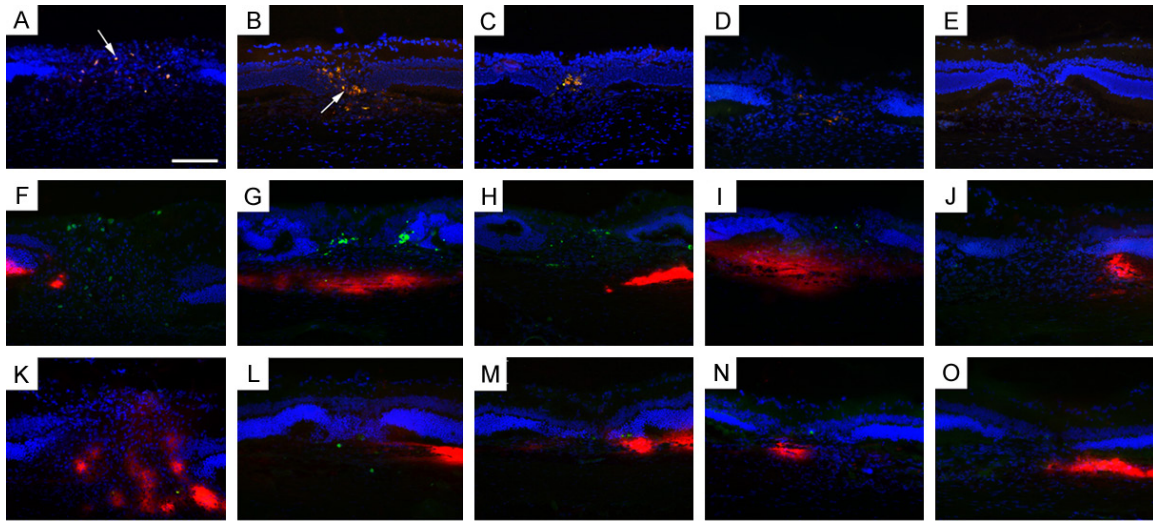


**Figure 3.** Tissue localization of apelin and RFP by immunofluorescence staining in the CNV model from day 3 to day 28 after photocoagulation. (A-E) The yellow fluorescence (arrowheads) resulted from the co-localization of apelin (green fluorescence) and CD105 (red fluorescence; see [Figure S1](#)). (F-O) The green fluorescence and red fluorescence arose from apelin and RFP, respectively (see [Figure S2](#)). The expression of apelin in the Vehicle group increased on day 3 after photocoagulation (A), reached its maximum around day 7 (B), and then decreased (C-E). Although red fluorescence of RFP was shown in the sections from the NC group, the apelin in the NC group (F-J) was expressed in the same manner as it in the Vehicle group. However, in the RNAi group, the expression of apelin was suppressed significantly from day 3 to day 14 (K-M). Scale bar = 100  $\mu\text{m}$ .

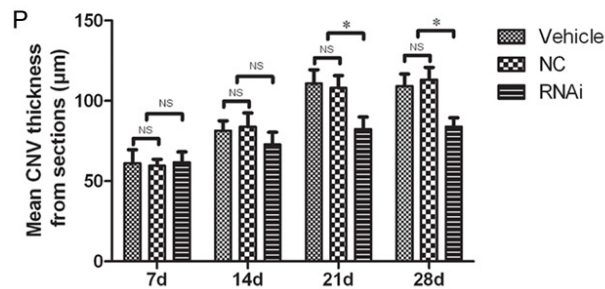
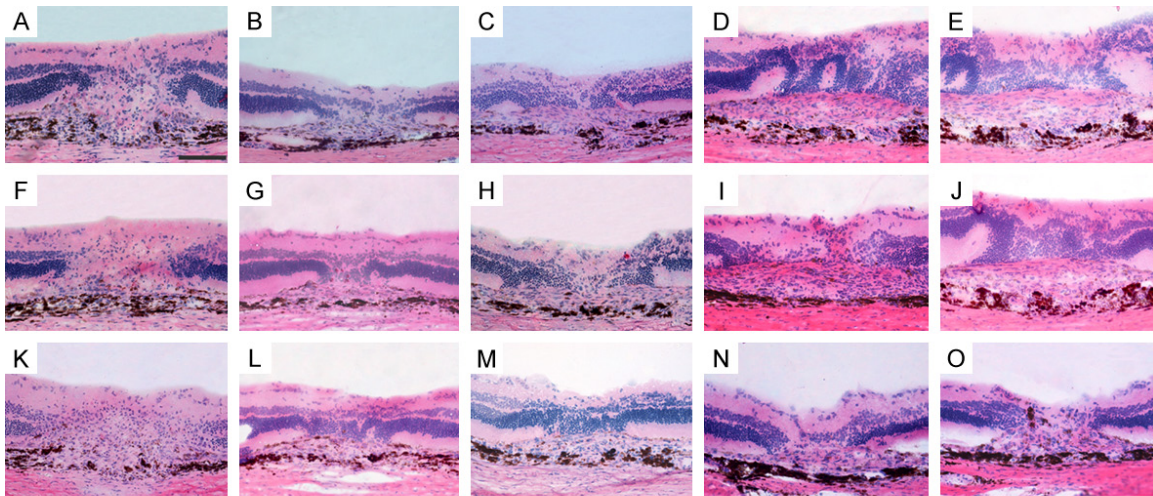


**Figure 4.** Light micrographs of H-E stained sections of the CNV tissue from day 3 to day 28 after photocoagulation. (A-E) Vehicle group, (F-J) NC group, (K-O) RNAi group. The measurement and comparison of the CNV thickness from the histopathological section yielded (P). Data were expressed as the mean  $\pm$  SEM. \* $P < 0.05$ .

could downregulate the expression of apelin after the intravitreal injection of lentivirus. The

intravitreal injection with Apelin-RNAi-LV resulted in significant suppression of apelin expres-

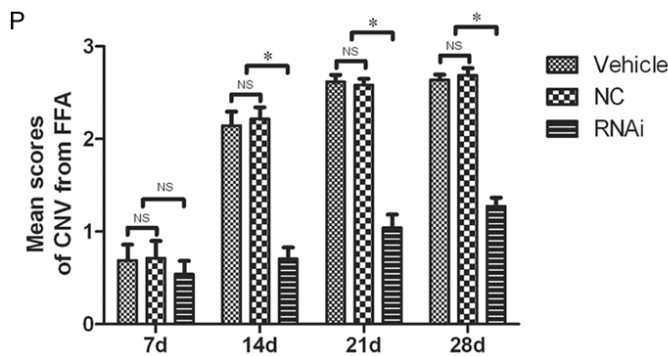
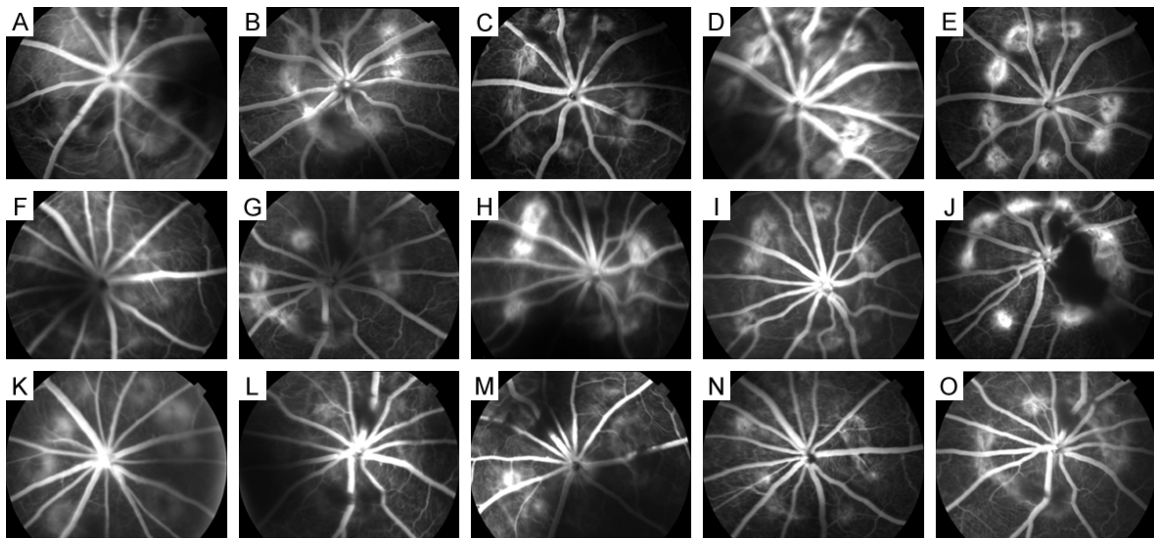


**Figure 5.** FFA of laser-induced CNV from day 3 to day 28 after photocoagulation. (A-E) Vehicle group, (F-J) NC group, (K-O) RNAi group. CNV emerged on day 7 after photocoagulation (B, G, and L). From day 7, CNV in the Vehicle group (B-E) and NS group (G-J) showed moderate to severe fluorescein leakage; however, CNV in RNAi group (L-O) showed slight fluorescein leakage. There was a statistically significant difference in the CNV mean scores from day 14 after photocoagulation (P). \* $P < 0.05$ .

sion in the RNAi group from day 3 to day 14 after photocoagulation (Figures 1C, 1D, 2C and 2D). In the NC group, apelin was expressed in the same manner as in the Vehicle group (Figures 1B and 1D, 2B and 2D), indicating that intravitreal injection with NC-RFP-LV did not affect its expression.

*Tissue localization of apelin and RFP after intravitreal injections of lentivirus in the CNV model*

To further confirm the tissue localization of apelin and RFP after the intravitreal injection of lentivirus, immunofluorescence staining was performed. Frozen sections from the Vehicle group showed no fluorescence of RFP at any time point (Figure 3A-E). Frozen sections from the NC group and RNAi group showed red fluorescence of RFP as early as 3 days after intravitreal injection, and it remained until day 28 at least (Figure 3F-O; the method that yielded the merged pictures see Figure S2).

In the RNAi group, the expression of apelin was suppressed significantly from day 3 to day 14 (Figure 3K-M), suggesting that the Apelin-RNAi-

LV silenced the apelin gene in this study. Although the sections from the NC group showed red fluorescence of RFP, apelin was expressed in the same manner as in the Vehicle group (Figure 3F-J).

*Silencing of apelin inhibited the development of CNV*

Experiments were next performed to investigate the effect of silencing apelin on the development of CNV tissue by the thickness of CNV from histopathological studies, the scores of CNV from FFA, and the area of CNV from the choroid flat mounts.

*Histopathological studies*

On day 7 after photocoagulation, a narrow CNV could be found to extend from the choroid into the subretinal space in histopathological sections (Figure 4B). The CNV thickness continued to increase from day 7 to day 28 after photocoagulation in the Vehicle group (Figure 4B-E) and in the NC group (Figure 4G-J), but it increased less obviously in the RNAi group from day 14 to day 28 (Figure 4L-P).

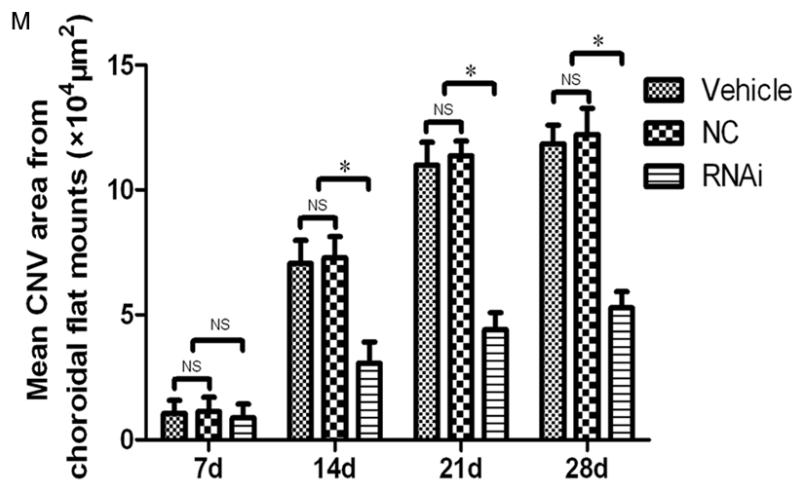
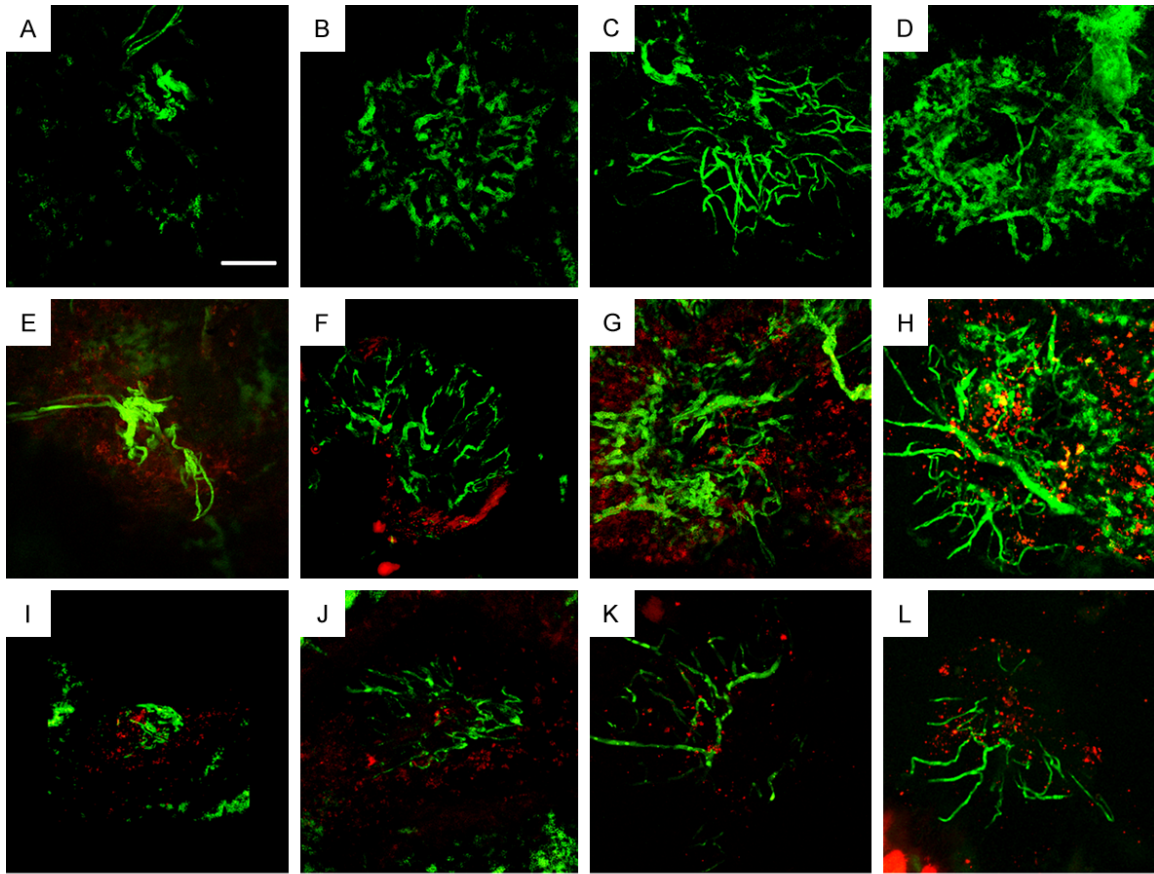


**Figure 6.** CNV labeled both FITC-dextran and RFP on choroid flat mounts from day 7 to day 28 after laser photocoagulation. The green fluorescence and red fluorescence arose from the CNV labeled with FITC-dextran and RFP respectively. The area of CNV increased dramatically from day 7 to day 21 in the Vehicle group (A-D) and the NC group (E-H), but less apparently in the RNAi group (I-L). The mean area of CNV in the RNAi group was less than that in the other groups from day 14 (M). Scale bar = 100 μm. Data were expressed as the mean ± SEM. \**P* < 0.05.

*FFA*

FFA showed slight fluorescein leakage but no CNV formation on day 3 after photocoagulation in the three groups (Figure 5A, 5F and 5K). Laser-induced lesions partially resulted in the emergence of CNV on day 7 (Figure 5B, 5G and 5L). From day 14, CNV in the Vehicle group (Figure 5C-E) and NS group (Figure 5H, 5J) showed moderate-to-severe fluorescein leakage, but CNV in the RNAi group (Figure 5M-O)

showed significantly lessened fluorescent leakage. There was a significant difference in the CNV mean scores among the three groups from day 14 (Figure 5P).

*FITC-dextran labeled choroid flat mounts*

The expression of RFP was clearly observed in the choroid flat mounts on day 7 in the NC group (Figure 6E-H) and RNAi group (Figure 6I-L). The area of CNV labeled with FITC-dextran

increased dramatically from day 7 to day 21 in the Vehicle group (**Figure 6A-C**) and NC group (**Figure 6E-G**), but less apparently in the RNAi group (**Figure 6I-K**). The mean area of CNV in the RNAi group was smaller than that in the other groups from day 14 after photocoagulation (**Figure 6M**).

### Discussion

Untreated CNV leads to the loss of central vision and thus has a profound impact on the quality of life. Therefore, various experimental CNV models have been developed to investigate its molecular mechanism. Apelin is reported to be an angiogenic factor, and its function cannot be replaced by VEGF [10]. Our previous studies have demonstrated that apelin may be involved in retinal neovascularization during the development of proliferative diabetic retinopathy and central retinal vein occlusion [11, 16]. In this study, we attempt to demonstrate the role of apelin in laser-induced CNV model.

In the present study by FFA, histopathological sections and FITC-dextran-labeled choroid flat mounts, we described the natural history of laser-induced CNV. Briefly, the experimental CNV occurred on around day 7 after photocoagulation, kept increasing in thickness (**Figure 4**), FFA scores (**Figure 5**), and area (**Figure 6**), and reached a stable state on day 21, remaining stable for 1 week at least. The natural history of laser-induced CNV in our study was similar to that demonstrated in previous study [15].

CD105 has been considered a marker of actively proliferating ECs [14, 17]. By the immunofluorescence method, we demonstrated that apelin was co-expressed with CD105 in the activated ECs in the experimental CNV model (**Figure 3A-E**). Previous experiments had also implied that ECs might be the most important source of apelin [13, 18, 19]. In the present study, we confirmed it was the actively proliferating ECs that apelin was mainly expressed in. Similar to the results from RT-PCR and western-blot analysis, the expression of apelin in the frozen sections with immunofluorescent staining was upregulated on day 3, reached the maximum on day 7 after photocoagulation, and then decreased (**Figure 3A-E**).

In our study, we observed that both the mRNA and protein levels of apelin were upregulated in the experimental CNV model in a time-depen-

dent manner (**Figures 1A** and **2A**). And then, to further confirm the possible role of the apelin, it was necessary to investigate the influence by silencing apelin in the CNV model. After silencing the apelin gene by intravitreal injection of lentivirus, the expression of apelin was significantly downregulated (**Figures 1C, 1D, 2C** and **2D**), and the development of CNV was suppressed, as observed by the CNV thickness from histopathological studies (**Figure 4**), scores of CNV from FFA (**Figure 5**), and area of CNV from the choroid flat mounts (**Figure 6**). Based on these findings, we concluded that the apelin might play an important role in the development of laser-induced CNV.

In conclusion, our results demonstrate that the apelin is involved in the development of laser-induced CNV and that silencing apelin can suppress the development of CNV significantly. Based on our findings, we postulate that apelin plays an important role in CNV formation, and it may act as a novel therapeutic option to inhibit CNV.

### Acknowledgements

This study was supported by Beijing Natural Science Foundation (No. 7112142), Research Fund for the Doctoral Program of Higher Education of China (No. 20100001110073; No. 20110001110042), and National Natural Science Foundation of China (No. 81271027).

### Disclosure of conflict of interest

None.

**Address correspondence to:** Jiang Yanrong, Department of Ophthalmology, People's Hospital, Peking University; Key Laboratory of Vision Loss and Restoration, Ministry of Education; Beijing Key Laboratory of Diagnosis and Therapy of Retinal and Choroid Diseases, 11 Xizhimen South Street, Xicheng District, Beijing 100044, China. Tel: + 86-10-88325413; Fax: + 86-10-88395310; E-mail: drjyr@vip.sina.com

### References

- [1] Grossniklaus HE, Kang SJ and Berglin L. Animal models of choroidal and retinal neovascularization. *Prog Retin Eye Res* 2010; 29: 500-519.
- [2] Jager RD, Mieler WF and Miller JW. Age-related macular degeneration. *N Engl J Med* 2008; 358: 2606-2617.

## Apelin is essential for CNV

- [3] Schwesinger C, Yee C, Rohan RM, Joussem AM, Fernandez A, Meyer TN, Poulaki V, Ma JJ, Redmond TM, Liu S, Adamis AP and D'Amato RJ. Intrachoroidal neovascularization in transgenic mice overexpressing vascular endothelial growth factor in the retinal pigment epithelium. *Am J Pathol* 2001; 158: 1161-1172.
- [4] Lassota N, Kiilgaard JF, la Cour M, Scherfig E and Prause JU. Natural history of choroidal neovascularization after surgical induction in an animal model. *Acta Ophthalmol* 2008; 86: 495-503.
- [5] Jasielska M, Semkova I, Shi X, Schmidt K, Karagiannis D, Kokkinou D, Mackiewicz J, Kociok N and Joussem AM. Differential role of tumor necrosis factor (TNF)-alpha receptors in the development of choroidal neovascularization. *Invest Ophthalmol Vis Sci* 2010; 51: 3874-3883.
- [6] Lyzogubov VV, Tytarenko RG, Jha P, Liu J, Bora NS and Bora PS. Role of ocular complement factor H in a murine model of choroidal neovascularization. *Am J Pathol* 2010; 177: 1870-1880.
- [7] Amaral J and Becerra SP. Effects of human recombinant PEDF protein and PEDF-derived peptide 34-mer on choroidal neovascularization. *Invest Ophthalmol Vis Sci* 2010; 51: 1318-1326.
- [8] Tatemoto K, Hosoya M, Habata Y, Fujii R, Kakegawa T, Zou MX, Kawamata Y, Fukusumi S, Hinuma S, Kitada C, Kurokawa T, Onda H and Fujino M. Isolation and characterization of a novel endogenous peptide ligand for the human APJ receptor. *Biochem Biophys Res Commun* 1998; 251: 471-476.
- [9] Kasai A, Shintani N, Oda M, Kakuda M, Hashimoto H, Matsuda T, Hinuma S and Baba A. Apelin is a novel angiogenic factor in retinal endothelial cells. *Biochem Biophys Res Commun* 2004; 325: 395-400.
- [10] Kalin RE, Kretz MP, Meyer AM, Kispert A, Heppner FL and Brandli AW. Paracrine and autocrine mechanisms of apelin signaling govern embryonic and tumor angiogenesis. *DEV BIOL* 2007; 305: 599-614.
- [11] Tao Y, Lu Q, Jiang YR, Qian J, Wang JY, Gao L and Jonas JB. Apelin in plasma and vitreous and in fibrovascular retinal membranes of patients with proliferative diabetic retinopathy. *Invest Ophthalmol Vis Sci* 2010; 51: 4237-4242.
- [12] Qin D, Zheng XX and Jiang YR. Apelin-13 induces proliferation, migration, and collagen I mRNA expression in human RPE cells via PI3K/Akt and MEK/Erk signaling pathways. *Mol Vis* 2013; 19: 2227-2236.
- [13] Kasai A, Ishimaru Y, Kinjo T, Satooka T, Matsumoto N, Yoshioka Y, Yamamuro A, Gomi F, Shintani N, Baba A and Maeda S. Apelin is a crucial factor for hypoxia-induced retinal angiogenesis. *Arterioscler Thromb Vasc Biol* 2010; 30: 2182-2187.
- [14] Semkova I, Fauser S, Lappas A, Smyth N, Kociok N, Kirchhof B, Paulsson M, Poulaki V and Joussem AM. Overexpression of FasL in retinal pigment epithelial cells reduces choroidal neovascularization. *FASEB J* 2006; 20: 1689-1691.
- [15] Edelman JL and Castro MR. Quantitative image analysis of laser-induced choroidal neovascularization in rat. *Exp Eye Res* 2000; 71: 523-533.
- [16] Zhao T, Lu Q, Tao Y, Liang XY, Wang K and Jiang YR. Effects of apelin and vascular endothelial growth factor on central retinal vein occlusion in monkey eyes intravitreally injected with bevacizumab: a preliminary study. *Mol Vis* 2011; 17: 1044-1055.
- [17] Nassiri F, Cusimano MD, Scheithauer BW, Rotondo F, Fazio A, Yousef GM, Syro LV, Kovacs K and Lloyd RV. Endoglin (CD105): a review of its role in angiogenesis and tumor diagnosis, progression and therapy. *Anticancer Res* 2011; 31: 2283-2290.
- [18] Tiani C, Garcia-Pras E, Mejias M, de Gottardi A, Berzigotti A, Bosch J and Fernandez M. Apelin signaling modulates splanchnic angiogenesis and portosystemic collateral vessel formation in rats with portal hypertension. *J Hepatol* 2009; 50: 296-305.
- [19] Eyries M, Siegfried G, Ciumas M, Montagne K, Agrapart M, Lebrin F and Soubrier F. Hypoxia-induced apelin expression regulates endothelial cell proliferation and regenerative angiogenesis. *Circ Res* 2008; 103: 432-440.

Apelin is essential for CNV

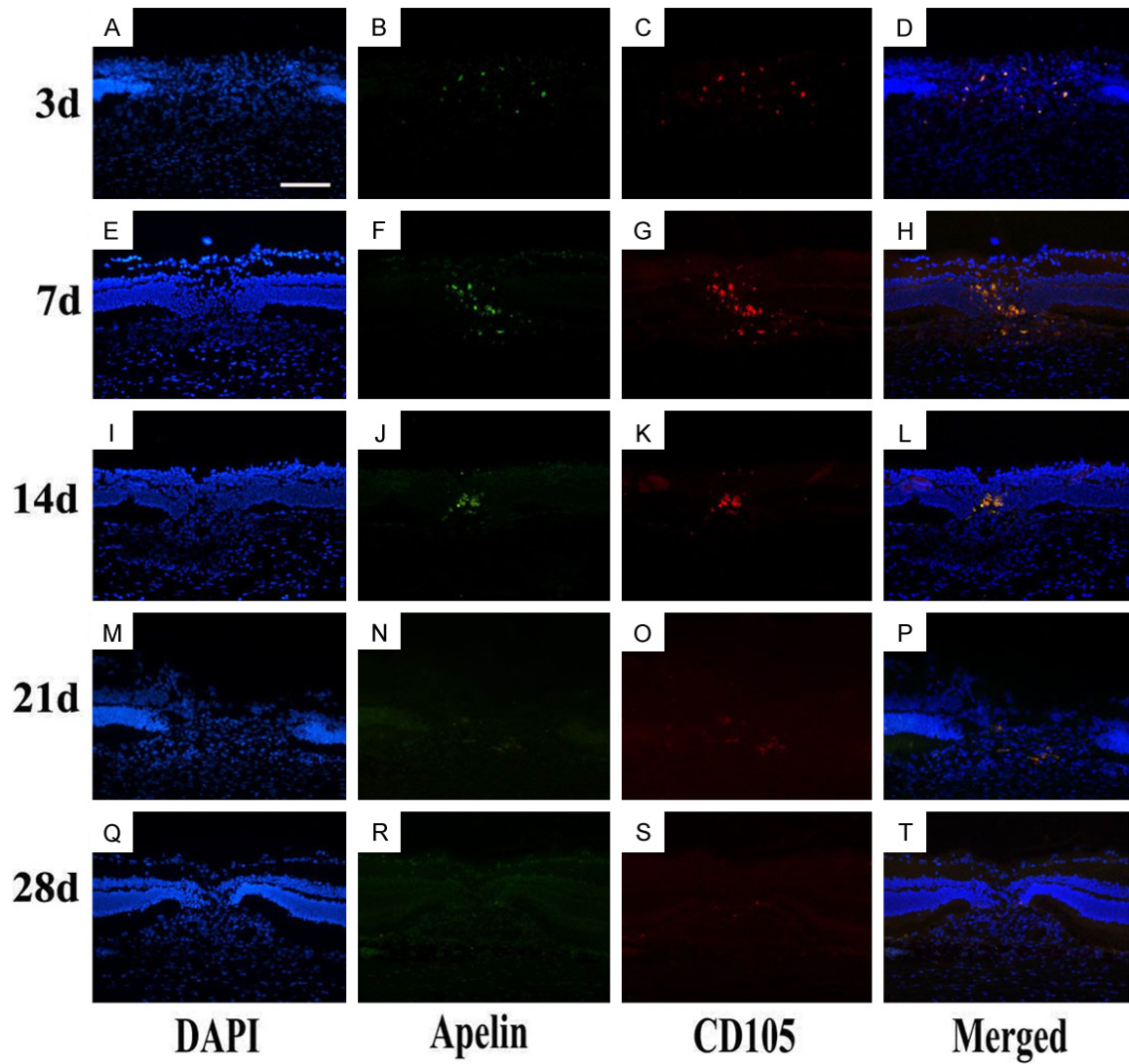


Figure S1. The method that yielded the merged Figure 3A-E.

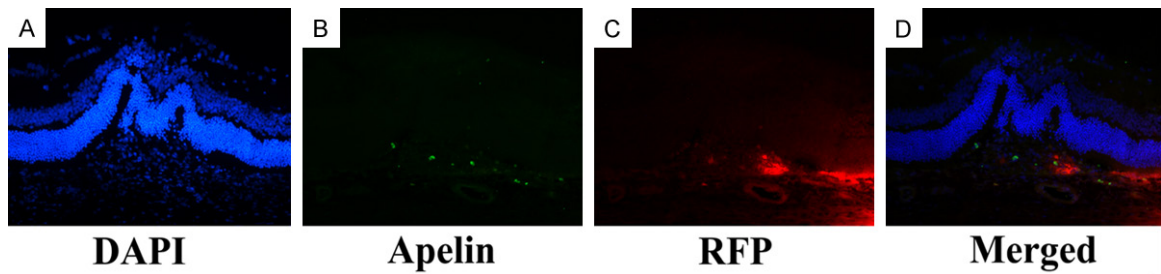


Figure S2. The method that yielded the merged Figure 3F-O.